multimedia

Monitoring of exocytosis and endocytosis of insulin secretory granules in the pancreatic β-cell line MIN6 using pH-sensitive green fluorescent protein (pHluorin) and confocal laser microscopy

Mica OHARA-IMAIZUMI*, Yoko NAKAMICHI*, Toshiaki TANAKA†, Hidenori KATSUTA†, Hitoshi ISHIDA† and Shinya NAGAMATSU*[1]

*Department of Biochemistry, Kyorin University School of Medicine, Mitaka, Tokyo 181-8611, Japan, and †Department of Internal Medicine (III), Kyorin University School of Medicine, Mitaka, Tokyo 181-8611, Japan

The dynamics of exocytosis/endocytosis of insulin secretory granules in pancreatic β-cells remains to be clarified. In the present study, we visualized and analysed the motion of insulin secretory granules in MIN6 cells using pH-sensitive green fluorescent protein (pHluorin) fused to either insulin or the vesicle membrane protein, phogrin. In order to monitor insulin exocytosis, pHluorin, which is brightly fluorescent at approximately pH 7.4, but not at approximately pH 5.0, was attached to the C-terminus of insulin. To monitor the motion of insulin secretory granules throughout exocytosis/endocytosis, pHluorin was inserted between the third and fourth amino acids after the identified signal-peptide cleavage site of rat phogrin cDNA. Using this method of cDNA construction, pHluorin was located in the vesicle lumen, which may enable discrimination of the unfused acidic secretory granules from the fused neutralized ones. In MIN6 cells expressing insulin–pHluorin, time-lapse confocal laser scanning microscopy (5 or 10 s intervals) revealed the appearance of fluorescent spots by depolarization after stimulation with 50 mM KCl and 22 mM glucose. The number of these spots in the image at the indicated times was counted and found to be consistent with the results of insulin release measured by RIA during the time course. In MIN6 cells expressing phogrin–pHluorin, data showed that fluorescent spots appeared following high KCl stimulation and remained stationary for a while, moved on the plasma membrane and then disappeared. Thus we demonstrate the visualized motion of insulin granule exocytosis/endocytosis using the pH-sensitive marker, pHluorin.

Key words: fusion, large dense-core granule, phogrin.

INTRODUCTION

Glucose is the most important regulatory factor for insulin secretion from pancreatic β-cells [1]. Glucose metabolism depolarizes β-cells by inhibiting the K_{ATP} channel [2,3], resulting in the increase of intracellular Ca^{2+} concentration ($[Ca^{2+}]_i$) by opening the voltage-dependent Ca^{2+} channel [4,5]. Insulin exocytosis by pancreatic β-cells is strictly controlled by $[Ca^{2+}]_i$ [6], although the detailed mechanism after $[Ca^{2+}]_i$ increase remains to be elucidated. Because the later stage of insulin exocytosis, associated with both $[Ca^{2+}]_i$ increase and soluble *N*-ethylmaleimide-sensitive fusion protein attachment protein receptor (SNARE) [7], must be involved in the regulation of insulin secretion, monitoring insulin secretory granule movement and the process of docking/fusion in living β-cells would be an effective method for determining the molecular mechanism in insulin exocytosis. However, tracing the movement of secretory granules has been a considerable technical challenge thus far. During the past decade, granule movement has been measured by fusing granule-membrane cargo proteins to fluorescent reporters [8,9]. However, a major problem with this approach is that only a few of the expressed fluorescent reporters are correctly targeted to mature secretory granules. Recently, Rutter and co-workers [10,11] used a construct generated by fusion between the phosphatase on the granule of insulinoma cells (phogrin), a dense-core secretory granule-membrane glycoprotein, and enhanced green fluorescent protein (EGFP) in order to monitor insulin granules. This protein chimaera was transported to insulin secretory granules and thus they succeeded in labelling and tracing these granules.

In the present study, we describe the exocytosis and endocytosis of insulin secretory granules from the pancreatic β-cell line MIN6 using the pH-sensitive GFP (pHluorin), a novel variant of GFP. Miesenbock et al. [12] originally developed ecliptic pHluorin, which is brightly fluorescent at approximately pH 7.4, but not at approximately pH 5.0. Because the mature insulin secretory granules maintain an acidic lumen (pH 5.0–5.5) [13], resulting from the activity of a vacuolar H^+-ATPase [14], pHluorin targeted to the insulin secretory granule lumen enables discrimination between fused and unfused granules. This is possible because, after the fusion with the plasma membrane by secretagogue stimulation, the pH of the granule lumen becomes alkaline in the extracellular environment (approximately pH 7.4). To label the insulin secretory granules, we have constructed two kinds of chimaeric cDNAs: (1) phogrin–pHluorin, which is produced by fusion between rat phogrin and pHluorin, where pHluorin was located on the luminal side of the vesicle; and (2) insulin–pHluorin, where pHluorin was attached to the C-terminus of human prepro-insulin. Using these cDNA constructs, our data demonstrate the visualization of exocytosis/endocytosis of insulin secretory granules in pancreatic β-cells.

Abbreviations used: $[Ca^{2+}]_i$, intracellular calcium concentration; (E)GFP, (enhanced) green fluorescent protein; pHluorin, pH-sensitive GFP; phogrin, phosphatase on the granule of insulinoma cells; KRB, Krebs–Ringer buffer; RFP, rhodamine fluorescent protein; SNARE, *N*-ethylmaleimide-sensitive fusion protein attachment protein receptor.

[1] To whom correspondence should be addressed (e-mail shinya@kyorin-u.ac.jp).

MATERIALS AND METHODS

Materials

Expression vectors, such as pEGFP, pEYFP and pDsRed, were obtained from ClonTech Laboratories (Palo Alto, CA, U.S.A.). pGEM™-Easy and pCI-neo mammalian expression vectors were from Promega (Madison, WI, U.S.A.). *Taq* DNA polymerase and the Mutan™-Super Express Km mutagenesis kit were purchased from TaKaRa Shuzo Co. (Shiga, Japan). Effecten™ reagent was from Qiagen GmbH (Hilden, Germany).

Plasmid construction

For the construction of the chimaeric protein between insulin and pHluorin (insulin–pHluorin), the PCR-amplified coding region lacking the stop codon of human prepro-insulin cDNA (a gift from Dr G. I. Bell, Howard Hughes Medical Institute, University of Chicago, Chicago, IL, U.S.A.) was cloned into the corresponding region of pEYFP-N1 vector. The coding region of yellow fluorescent protein ('YFP') was then replaced by ecliptic pHluorin. The fusion cDNA between human insulin and rhodamine fluorescent protein (RFP) (insulin–RFP) was produced by a similar method using the pDsRed-N1 vector. For the construction of the chimaeric phogrin–pHluorin protein, cDNA encoding the entire coding region of rat phogrin (a generous gift from Dr J. C. Hutton, Barbara Davis Center for Childhood Diabetes, University of Colorado Health Sciences Center, Denver, CO, U.S.A.), including a Kozak sequence, was digested with *Bam*HI, and the resulting cDNA fragment containing the 5′ region was subcloned into the plasmid pKF18K (TaKaRa Shuzo Co.) to allow the mutagenesis of the construct. Because the phogrin has dibasic residues (Lys^{414} and Lys^{415}) on the luminal side, which must be cleaved in mature insulin secretory granules [15], Lys^{414} and Lys^{415} were mutated to Asn^{414} and Asn^{415} to prevent proteolytic processing; therefore phogrin–pHluorin is bound to the vesicle membrane throughout exocytosis and endocytosis. Mutagenesis was carried out according to the manufacturer's instructions, and the mutation was confirmed using an automated sequencer (Gene Rapid; Amersham Biosciences, Little Chalfont, Bucks., U.K.). The signal peptide of rat phogrin, followed by three amino acids after the identified signal-peptide cleavage site, was attached to the N-terminus of ecliptic pHluorin (a generous gift from Dr J. Rothman, Cellular Biochemistry, Sloan-Kettering Institute, New York, NY, U.S.A.) by PCR. This was then attached immediately after the third amino acid residue after the signal-peptide cleavage site of truncated phogrin mutant. Finally, this chimaera cDNA was subcloned into the pCI-neo mammalian expression vector. All the PCR products were completely sequenced to ensure fidelity of construction. On the basis of our plasmid construct, as pHluorin is located in the vesicle lumen (Figure 1), resting vesicles, whose internal pH is below 5.5, are not visible at $\lambda_{excitation} = 488$ nm and only become fluorescent when they are fused with the plasma membrane and their internal pH increases to that of the extracellular space (approximately pH 7.4). This allows detection of individual vesicle-fusion events through bursts of fluorescent signals at $\lambda_{excitation} = 488$ nm.

Cell culture and transfection

MIN6 cells (a gift from Dr J.-i. Miyazaki, Department of Molecular Medicine, Osaka University, Osaka, Japan) at passage 15–35 were maintained in Dulbecco's modified Eagle's medium containing 10% (v/v) foetal-bovine serum and 28.4 μM 2-mercaptoethanol in an atmosphere of 5% CO_2 at 37 °C. For *in vivo* confocal imaging experiments, cells were divided, grown on LAB-TEK chamber slides (Nalge Nunc International, Naperville, IL, U.S.A.), and transfected with the recombinant expression vectors using Effecten™ (Qiagen).

Immunofluorescence microscopy

For immunofluorescent studies of MIN6 cells, cells were grown on coverslips for 2 days and then transfected with the required expression vectors. Cells were fixed with 2% paraformaldehyde, immunostained with a monoclonal anti-insulin antibody (Sigma, St. Louis, MO, U.S.A.), and examined using laser scanning confocal microscopy (LSM510; Carl Zeiss Co., Jena, Germany), as described previously [16].

Confocal imaging analysis

Prior to imaging, cells were incubated for 30 min in Krebs–Ringer buffer [KRB: 110 mM NaCl, 4.4 mM KCl, 2.3 mM $CaCl_2$, 1.45 mM KH_2PO_4, 1.2 mM $MgSO_4$, 4.83 mM $NaHCO_3$, 2.2 mM glucose, 10 mM Hepes (pH 7.4)] containing 0.3% (v/v) BSA. Cells were then transferred on to the thermostat-controlled (37 °C) stage of a Zeiss laser scanning confocal microscope (LSM 510). The cells were stimulated with a high K^+ solution (KRB containing 50 mM KCl and 7.2 mM NaCl, prewarmed to 37 °C) and/or 22 mM glucose in KRB when required. The time course of the fluorescence response of insulin–pHluorin or phogrin–pHluorin was obtained from time-lapse images every 5 or 10 s during stimulation at a $\lambda_{excitation} = 488$ nm. In order to avoid the vesicular lysis by bright-laser illumination, we used a minimal

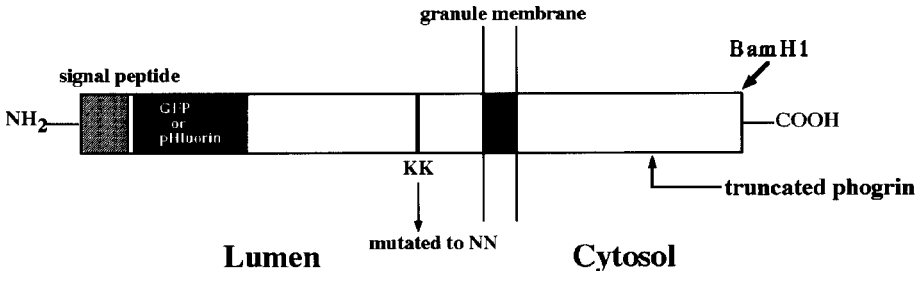

Figure 1 Construction of the chimaeric protein between phogrin and pHluorin

Full-length cDNA of rat phogrin was digested with *Bam*HI. The truncated phogrin was ligated into the pKF18K vector to substitute the dibasic residues Lys^{414} and Lys^{415} with Asn. EGFP or pHluorin was then inserted between the third and fourth amino acids after the identified signal-peptide cleavage site of the truncated mutated phogrin by standard molecular biological techniques using the pCI-neo mammalian expression vector.

laser power. In fact, the decrease of fluorescent intensities of pHluorin due to photobleaching was less than 10 % over 10 min. Quantitative measurements of fluorescent intensity and detailed analysis were performed using MetaMorph imaging software (Universal Imaging, West Chester, PA, U.S.A.). For the experiment examining the granule pH, NH_4Cl solution (pH 7.4) was prepared by substituting 50 mM NaCl with 50 mM NH_4Cl, with all other components remaining unchanged. The cells expressing phogrin–pHluorin were exposed to NH_4Cl (50 mM final concentration) in KRB, and the time course of fluorescence change was measured.

Insulin release

MIN6 cells were grown in 24-well multiplates (1×10^4 cells/well) and incubated in KRB containing low glucose (2.2 mM glucose) for 30 min before the stimulation. Cells were then challenged with KRB containing either 2.2 mM glucose, 50 mM KCl or 22 mM glucose for the indicated time. The medium was collected at 1 min intervals, and immunoreactive insulin was analysed by RIA.

RESULTS AND DISCUSSION

Cellular localization of chimaeric protein expressed in MIN6 cells

Before the use of chimaeric insulin–pHluorin and phogrin–pHluorin fusion proteins as probes to label insulin secretory granules, we determined if these proteins were localized precisely to insulin secretory granules. For the purpose of visualizing the cellular localization of phogrin–pHluorin, we constructed chimaeric cDNA by fusing phogrin and EGFP, with EGFP being in the same position as pHluorin in the phogrin–pHluorin construct (Figure 1). To determine if phogrin–EGFP was localized in the insulin secretory granules, MIN6 cells were first transfected with the phogrin–EGFP expression vector, and then were immunostained with the anti-insulin antibody. As shown in Figure 2 (upper panel), vesicular distribution of EGFP (phogrin) was consistent with insulin signals, which were detected by a rhodamine-labelled antibody, indicating that phogrin–EGFP was localized in the insulin secretory granules.

We next attempted to examine the cellular localization of insulin–pHluorin. For this, we produced insulin–RFP by fusion between RFP and the C-terminus of human prepro-insulin, with RFP being in exactly the same position as the insulin–pHluorin construct. MIN6 cells were co-transfected with both phogrin–EGFP and insulin–RFP. After 48 h, transfected cells were observed with confocal laser microscopy using a band-pass filter to avoid the overlap of the two wavelengths. Figure 2 (lower panel) clearly demonstrates the co-localization of phogrin (EGFP) and insulin (RFP) signals, suggesting that insulin–pHluorin was transported to the insulin secretory granules.

Insulin exocytosis visualized by insulin–pHluorin

We attempted to monitor insulin exocytosis stimulated by 50 mM KCl and the fuel secretagogue, glucose (22 mM), in MIN6 cells expressing insulin–pHluorin by time-lapse confocal imaging. Because pHluorin only emits bright fluorescence when insulin–pHluorin is exposed to neutral pH conditions, the appearance of a fluorescent spot after secretagogue stimulation is thought to equal either the formation of a fusion pore or insulin–pHluorin release from the vesicle. Figure 3(B) shows time-lapse images every 5 s for up to 245 s, corresponding to the boxed image (image 1) in Figure 3(A), and reveals that fluorescent signals

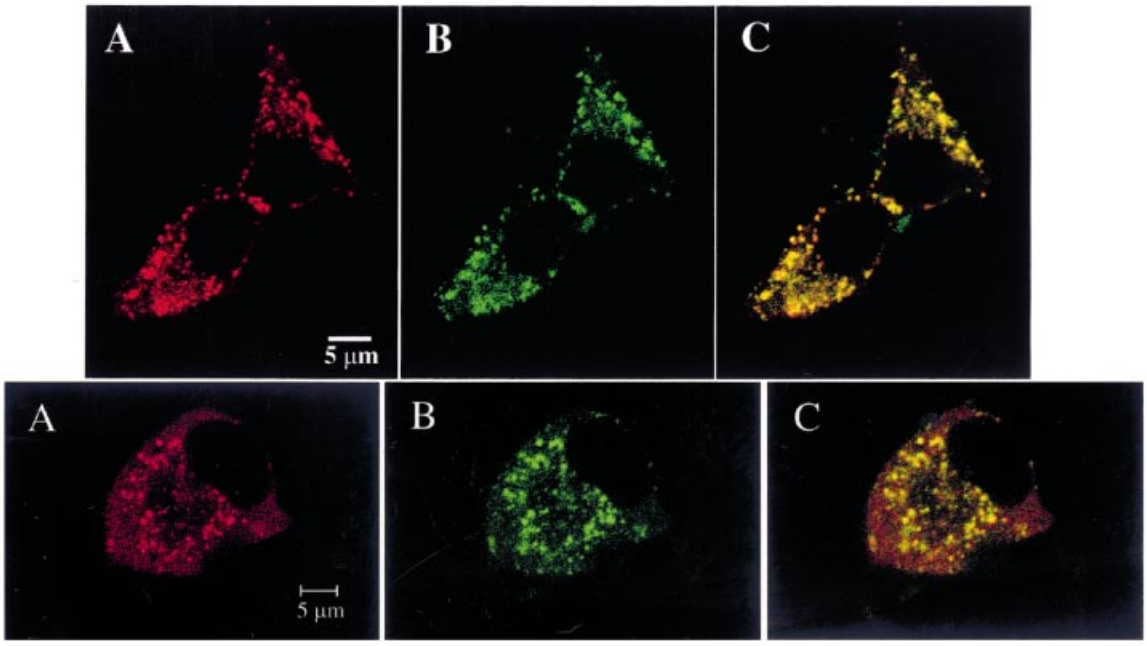

Figure 2 Localization of phogrin–EGFP and insulin–RFP in MIN6 cells

Upper panel: localization of phogrin–EGFP in insulin secretory granules. After 2 days, MIN6 cells were transfected with phogrin–EGFP expression vector, cells were fixed and immunostained with an anti-insulin antibody. Antibody complexes were visualized with the appropriate secondary antibody coupled to rhodamine. A striking co-localization (C, yellow) between phogrin–EGFP (B, green) and insulin (A, red) is shown. To avoid overlapping the fluorescent signal from rhodamine and FITC during laser scanning microscopy, a band-pass filter was used. Lower panel: co-localization of insulin–RFP and phogrin–EGFP. MIN6 cells were transfected with both insulin–RFP and phogrin–EGFP expression vectors, and 2 days later, cells were observed with confocal laser-scanning microscopy with an $\lambda_{excitation} = 488$ nm for EGFP and $\lambda_{excitation} = 543$ nm for RFP, with a band-pass filter. A striking co-localization (C, yellow) between insulin–RFP (A, red) and phogrin–EGFP (B, green) is shown. Scale bar, 5 μm.

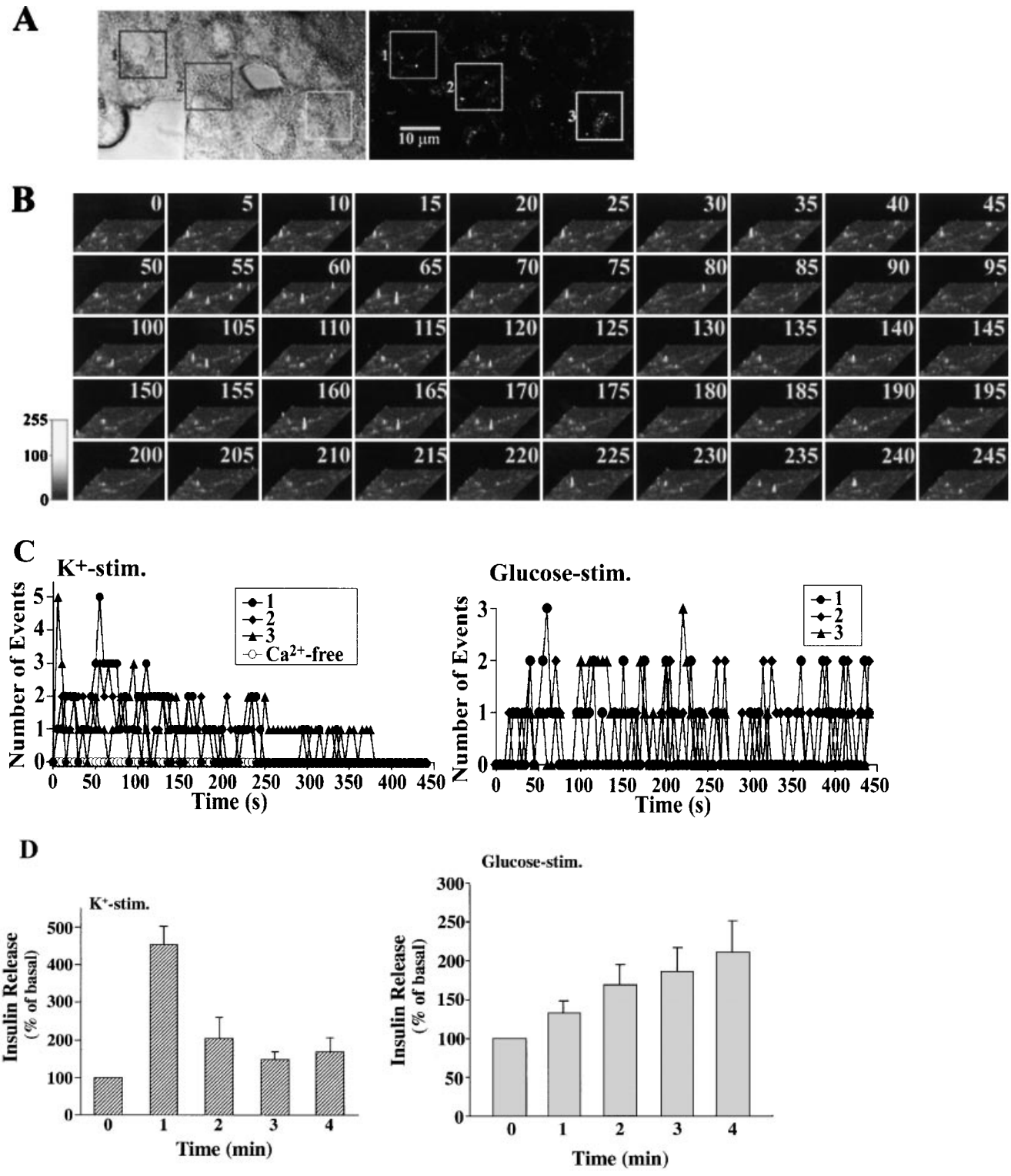

Figure 3 Time-lapse images of 50 mM KCl- and 22 mM glucose-induced exocytosis of insulin–pHluorin

(**A**) Nomarski (left) and fluorescent (right) images of MIN6 cells in culture maintained in 2.2 mM glucose. Boxed area 1 corresponds to time-lapse images shown in (**B**). (**B**) Time-lapse images of fluorescent spots of insulin–pHluorin induced by stimulation with 50 mM KCl. MIN6 cells expressing insulin–pHluorin were preincubated for 30 min with 2.2 mM glucose, and then were challenged with 50 mM KCl. Fluorescent images were obtained every 5 s up to 245 s by confocal laser microscopy, and the number shown in each image represents the time (s). Images were analysed with the MetaMorph imaging software. Fluorescent intensity is shown in black and white, with strong intensities being white, as indicated in the bar on the left. Brighter spots shown in white represent vesicle fusion. Part of these images is also presented as a time-lapse movie (movie 1, which is available at http://www.BiochemJ.org/bj/363/bj3630073add.htm). Time 0 indicates the addition of 50 mM KCl. (**C**) Number of fluorescent spots (fusion events) in each frame sequence following KCl (K^+-stim.) and glucose (Glucose-stim.) stimulation. For KCl treatment, the number of brighter spots (white) shown in (**B**) was counted as fusion events/5 s and plotted against time. Each line (1, 2 and 3) corresponds to the boxed number shown in (**A**). For glucose treatment, MIN6 cells expressing insulin–pHluorin were stimulated with 22 mM glucose, and time-lapse images of fluorescent spots were obtained every 5 s for up to 410 s. The number of bright spots

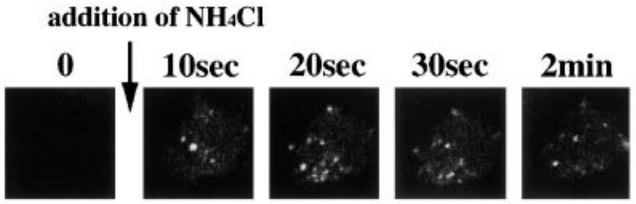

Figure 4 Increase in phogrin–pHluorin fluorescence following exposure to NH_4Cl

MIN6 cells were transfected with the phogrin–pHluorin expression vector and, 2 days later, NH_4Cl (50 mM final concentration) was added to the culture medium. Fluorescent images were obtained after 10 s, 20 s, 30 s and 2 min.

appear immediately after stimulation with 50 mM KCl. The appearance of the fluorescence evoked by 50 mM KCl stimulation is visualized in movie 1 (which is available at http://www.BiochemJ.org/bj/363/bj3630073add.htm). We counted the appearance of bright fluorescent spots, shown in white in Figure 3(B), which were tentatively considered as fusion events. Since the number of fluorescent spots counted in each sequential frame every 5 s (Figure 3C; K^+-stim.) was consistent with the time course of insulin release into the medium as measured by RIA (Figure 3D; K^+-stim.), we attributed the fluorescent spots to be externalization of insulin–pHluorin via vesicle fusion with the plasma membrane. In Ca^{2+}-free medium, we did not observe any bright-fluorescent signals (Figure 3C, open circle), indicating that the fluorescence imaged was from the regulated pathway.

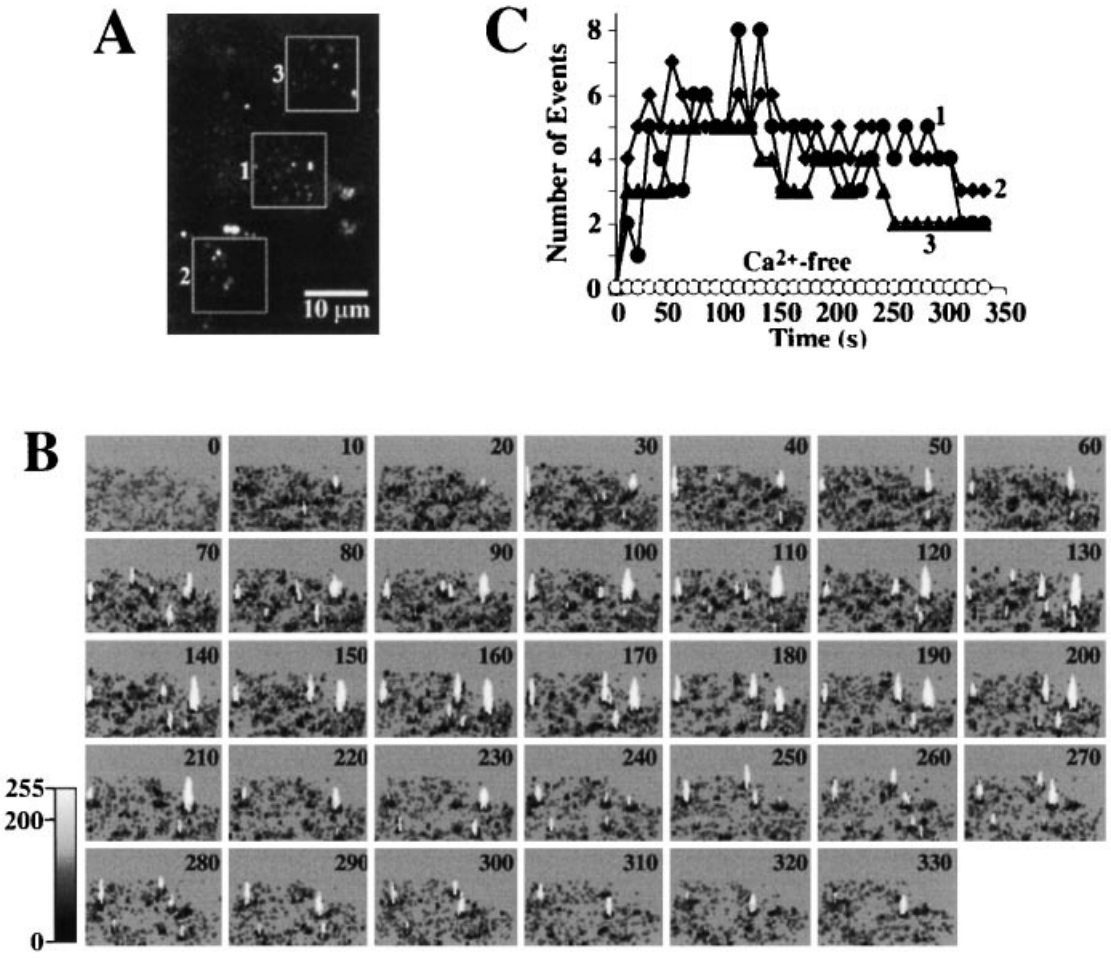

Figure 5 Time-course of phogrin–pHluorin fluorescent signals during stimulation with 50 mM KCl

(**A**) Fluorescent images of MIN6 cells harbouring phogrin–pHluorin prior to KCl stimulation. (**B**) Time-lapse images of phogrin–pHluorin fluorescence induced by stimulation with 50 mM KCl. MIN6 cells were challenged with 50 mM KCl, as in Figure 3. Fluorescent images in boxed area 1 were obtained every 10 s by confocal laser microscopy and obtained images were analysed. The number shown in each image is the time (s). Fluorescent intensity is shown in black and white, with strong intensities being white, as indicated in the bar on the left. Part of these images is also presented as a movie (movie 2, which is available at http://www.BiochemJ.org/bj/363/bj3630073add.htm). Time 0 indicates the addition of 50 mM KCl. (**C**) Number of fluorescent spots in each frame sequence. The number of fluorescent spots (fusion events) over threshold grey were counted and plotted against time. Each line (1, ●; 2, ◆; and 3, ▲) corresponds to the boxed number shown in (**A**). ○, number of fusion events in Ca^{2+}-free medium.

from three different regions were then counted. (**D**) Insulin release measured by RIA from MIN6 cells. MIN6 cells grown on 24-multiwell plates were incubated for 30 min with 2.2 mM glucose, and challenged with 50 mM KCl (K^+-stim.) or 22 mM glucose (Glucose-stim). Immunoreactive insulin in the medium was collected at 1 min intervals and assayed by RIA ($n = 4$). Results (means ± S.E.M.) are shown as the percentage of the basal value (time 0 in 2.2 mM glucose).

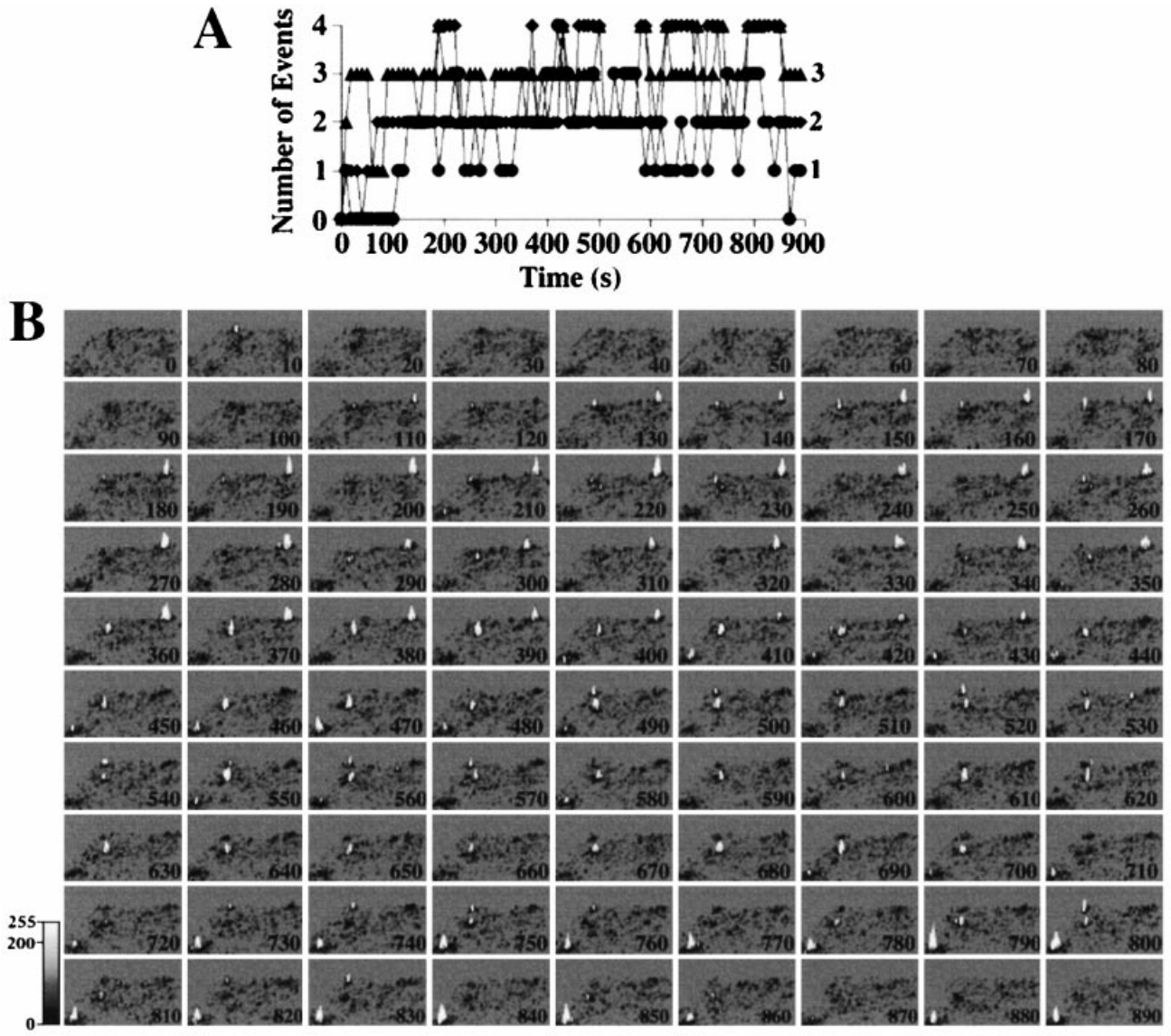

Figure 6 Time-course of phogrin–pHluorin signals during 22 mM glucose stimulation

(**A**) Number of fluorescent spots (fusion events). The number of brighter fluorescent spots (fusion events) threshold grey in each frame sequences shown in panel (**B**) was counted and plotted against time. Each line (1, ●; 2, ◆; and 3, ▲) represents the number counted from three different regions. (**B**) Representative time-lapse images of phogrin–pHluorin fluorescent signals stimulated by 22 mM glucose. MIN6 cells expressing phogrin–pHluorin were challenged with 22 mM glucose, and time-lapse images were obtained every 10 s for up to 890 s. Fluorescent intensity is shown in black and white, with strong intensities being white, as indicated in the bar on the left.

On the other hand, high glucose (22 mM) caused the continuous appearance of fluorescent signals during the stimulation. The number of fluorescent spots in each sequential frame (Figure 3C, Glucose-stim.) was generally constant during stimulation, which mostly agreed with the insulin-release data, as measured by RIA during the same time course (Figure 3D, Glucose-stim.). In the present study, we could not observe the spread and diffusion of the bright fluorescence of insulin–pHluorin, because the time scale of capturing the images with confocal laser microscopy was too slow to detect such a quick motion (ms order), as compared with studies reported by others using evanescent wave microscopy in non-β-cells [17,18].

It was noted that the fluorescent spots in Figure 3(B) remained in the same region throughout the 5 s frame sequences. This may indicate: (1) the existence of an active zone of vesicle fusion events in pancreatic β-cells, as observed in neuronal cells [19,20], such that insulin secretory granules may be fused in the same region one after another; and (2) the phenomenon of flicker [21], where transient opening and closing of a fusion pore would change the vesicle's internal pH, and thus affect pHluorin emission. Since the number of fluorescent spots in each frame during secretagogue stimulation was in good agreement with the time course of insulin release, as measured by RIA, we support the former possibility.

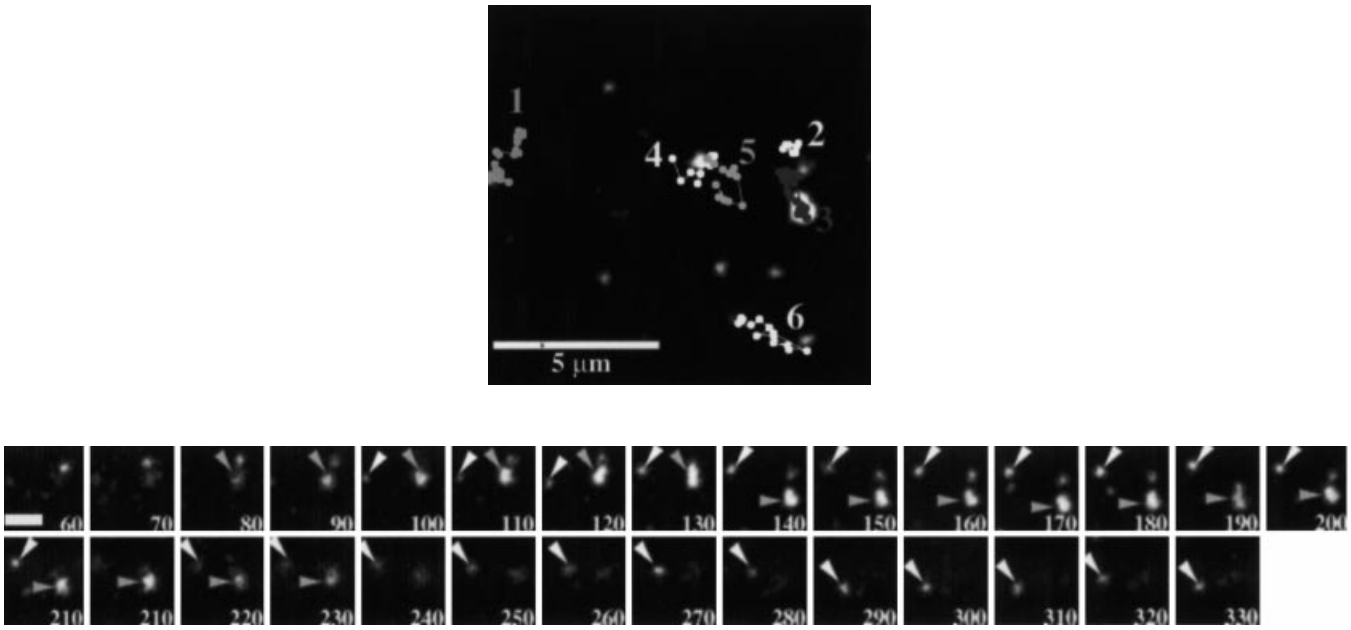

Figure 7 Exocytosis/endocytosis of individual insulin secretory granules

MIN6 cells expressing phogrin–pHluorin were challenged with 50 mM KCl, and time-lapse fluorescent images were taken every 10 s for up to 330 s. Upper panel: movement of the single fluorescent spots was tracked. Lower panel: the single fluorescent spots were monitored throughout their appearance and disappearance. The number shown in each image is the time (s). Scale bar, 1 μm. All image analysis was performed using MetaMorf imaging software.

Time-lapse images of exocytosis of insulin secretory granules labelled with phogrin–pHluorin by stimulation with 50 mM KCl and 22 mM glucose

We now analysed the movement of insulin secretory granules by monitoring the appearance and disappearance of the fluorescent spots in MIN6 cells expressing phogrin–pHluorin after stimulation with secretagogues. Phogrin is an excellent marker for tracking the insulin secretory granule throughout exocytosis/endocytosis [22,23]. Because the signal peptide on the N-terminus of phogrin plays a crucial role in sorting this protein to dense-core secretory granules, we could not attach pHluorin to the N-terminus of phogrin. Therefore we inserted pHluorin between the third and fourth amino acids after the signal-peptide cleavage site of rat phogrin cDNA. This chimaeric protein, with the proteolytic cleavage site also mutated as described in the Materials and methods section, enabled us to use the phogrin–pHluorin as a probe for labelling insulin secretory granules. The most beneficial aspect of using the phogrin–pHluorin probe is that it allowed us not only to directly detect vesicle fusion, but also to track the internalization and re-acidification of the vesicle. Although the possibility cannot be ruled out that the change in phogrin–pHluorin fluorescence intensity represents an acidification during the maturation process of insulin secretory granules budding from the *trans*-Golgi network, our findings that there were no altered overall fluorescent signals under resting conditions (results not shown) and that increased fluorescent signals were only observed in high KCl- and high glucose-stimulated conditions (see movie 2, which is available at http://www.BiochemJ.org/bj/363/bj3630073add.htm), indicate that fluorescent spots probably reflect vesicle fusion. In addition, since it has not been reported that insulin granules in MIN6 cells are acidified, we examined if insulin granules are acidic compartments in MIN6 cells. To examine this, we applied NH_4Cl to alkalinize insulin granules, as ammonia is well known to diffuse across cell membranes and raise the secretory vesicle pH to 7.4 [12]. Application of NH_4Cl to MIN6 cells expressing phogrin–pHluorin led to a rapid increase in fluorescence (Figure 4), suggesting that insulin granules in MIN6 cells are acidified, thereby the fluorescence of phogrin–pHluorin is quenched within the granules.

After depolarization of MIN6 cells expressing phogrin–pHluorin with 50 mM KCl, fluorescent signals appeared rapidly with variable integrated intensity and gradually decayed with time (Figure 5B and movie 2, which is available at http://www.BiochemJ.org/bj/363/bj3630073add.htm). It should be noted that the appearance and disappearance of fluorescent spots by high K^+ stimulation was not caused by vesicular lysis by the bright-laser illumination, because the few fluorescent spots observed under non-stimulated conditions (2.2 mM glucose) remained stationary over 10 min (results not shown). Frame sequences in Figure 5(B) represent the time-lapse images (10 s intervals) of boxed area 1 shown in Figure 5(A), where the black colour of the fluorescent spot was depicted as a weak signal and the white colour as a strong one. After the intensities of the fluorescent spots reached a peak, they gradually decayed; however, some fluorescent spots suddenly appeared and then rapidly disappeared. The number of fluorescent spots above the grey-coloured threshold were counted tentatively as fusion events, and were plotted against time. Figure 5(C) shows that the number of fluorescent spots increased within 150 s, and gradually decreased, which agreed generally with the insulin release data shown in Figure 3(D) (K^+-stim.). The reason why the peak of the number of fluorescent spots was shifted to right may be due to the vesicles that merged with the membrane remaining stationary for a while without diffusing, whereas the fluorescent spots of insulin–pHluorin rapidly disappeared after their appearance by high KCl stimulation.

We have examined further the time-lapse fluorescence changes of phogrin–pHluorin following glucose (22 mM)-stimulated insulin granule fusion. Figure 6(B) shows the time-lapse images every 10 s for up to 890 s, demonstrating that the bright fluorescent spots started to appear 100 s after stimulation, and were continuously observed after this time. Figure 6(A) demonstrates the number of fluorescent spots in each sequential frame counted from three different regions; findings that are consistent with the insulin–pHluorin time-lapse image data shown in Figure 3(C) (Glucose-stim.).

Endocytosis of insulin secretory granules detected by phogrin–pHluorin

As shown in movie 2 (which is available at http://www.BiochemJ.org/bj/363/bj3630073add.htm), when MIN6 cells expressing phogrin–pHluorin were stimulated with 50 mM KCl, fluorescent spots appeared rapidly, with individual spots moving, and then disappearing. Therefore we investigated the movement of the single fluorescent spots by tracking them during the time course (Figure 7). Frame sequences (Figure 7, lower panel), where we have tracked a single spot, clearly depicted the appearance, moving and disappearance of the single spot after stimulation with 50 mM KCl. We attributed the disappearance of the fluorescent spot to insulin granule endocytosis followed by its re-acidification. Indeed, there is evidence that the endocytosed vesicle is very quickly acidified [24], and acid treatment quickly quenched the fluorescent signals in our system (results not shown). Sankaranarayanan and Ryan [25] described the exocytosis/endocytosis of synaptic vesicles with the same tool, in which the vesicle marker was pHluorin fused to VAMP-2 (a synaptic vesicle-specific SNARE protein), which is quenched by protons in the vesicles. They observed that fluorescence appeared upon vesicle fusion and faded rapidly after endocytosis. From Figure 7, the calculated mean time from the appearance (fusion) to disappearance (endocytosis) was 200 ± 15 s ($n = 15$). As shown in Figure 7 (upper panel), a fixed direction for the movement of the individual fluorescent spots on the plasma membrane was not observed.

Thus it is assumed that the exocytotic site is different from that of the endocytotic site in pancreatic β-cells, a finding also observed in synapses [26,27]. This phenomenon may represent evidence that the exocytotic machinery, such as SNARE proteins, is different from that of endocytotic machinery, such as dynamin [27], whose localization might be separated. However, further analysis of not only intracellular movement of insulin secretory granules, but also their movement beneath the plasma membrane is required, and is now under investigation.

In conclusion, we have reported the first demonstration of the dynamics of exocytosis/endocytosis of insulin secretory granules in living β-cells.

This study was supported by a Grant-in-Aid for Scientific Research (C)(11670148) from the Japanese Ministry of Education, Science and Culture, and grants from the Research for the Future Program from the Japan Society for the Promotion of Science (JSPS-RFTF97I00201), Research Fund of Mitsukoshi Health and Welfare Foundation, and the Japan Private School Promotion Foundation.

REFERENCES

1 Hedeskov, C. J. (1980) Mechanism of glucose-induced insulin secretion. Physiol. Rev. **60**, 442–509
2 Cook, D. L. and Hales, C. N. (1984) Intracellular ATP directly blocks K^+ channels in pancreatic B-cells. Nature (London) **311**, 271–273
3 Ashcroft, F. M., Harrison, D. E. and Ashcroft, S. J. H. (1984) Glucose induces closure of single potassium channels in isolated rat pancreatic β-cells. Nature (London) **312**, 446–448
4 Smith, P. A., Rorsman, P. and Ashcroft, F. M. (1989) Modulation of dihydropyridine-sensitive Ca^{2+} channels by glucose metabolism in mouse pancreatic β-cells. Nature (London) **342**, 550–553
5 Larsson, O., Kindmark, H., Brandstrom, R., Fredholm, B. and Berggren, P. O. (1996) Oscillations in K_{ATP} channel activity promote oscillations in cytoplasmic free Ca^{2+} concentration in the pancreatic β cell. Proc. Natl. Acad. Sci. U.S.A. **93**, 5161–5165
6 Wollheim, C. B. and Sharp, G. W. G. (1981) Regulation of insulin release by calcium. Physiol. Rev. **61**, 914–973
7 Wollheim, C. B., Lang, J. and Regazzi, R. (1996) The exocytotic process of insulin secretion and its regulation by Ca^{2+} and G-proteins. Diabetes Rev. **4**, 276–297
8 Heim, R., Cubitt, A. B. and Tsien, R. Y. (1995) Improved green fluorescence. Nature (London) **373**, 663–664
9 Pouli, A. E., Kennedy, H. J., Schofield, J. G. and Rutter, G. A. (1998) Insulin targeting to the regulated secretory pathway after fusion with green fluorescent protein and firefly luciferase. Biochem. J. **331**, 669–675
10 Pouli, A. E., Emmanouilidou, E., Zhao, C., Wasmeier, C., Hutton, J. C. and Rutter, G. A. (1998) Secretory-granule dynamics visualized *in vivo* with a phogrin–green fluorescent protein chimaera. Biochem. J. **333**, 193–199
11 Tsuboi, T., Zhao, C., Terakawa, S. and Rutter, G. A. (2000) Simultaneous evanescent wave imaging of insulin vesicle membrane and cargo during a single exocytotic event. Curr. Biol. **10**, 1307–1310
12 Miesenbock, G., DeAngelis, D. A. and Rothman, J. E. (1998) Visualizing secretion and synaptic transmission with pH-sensitive green fluorescent proteins. Nature (London) **394**, 192–195
13 Orci, L. (1985) The insulin factory: a tour of the plant surroundings and a visit to the assembly line. Diabetologia **28**, 528–546
14 Hutton, J. C. (1982) The internal pH and membrane of the insulin-secretory granule. Biochem. J. **204**, 171–178
15 Hawkes, C. J., Wasmeier, C., Christie, M. R. and Hutton, J. C. (1996) Identification of 37-kDa antigen in IDDM as a tyrosine phosphatase-like protein phogrin related to IA-2. Diabetes **45**, 1187–1192
16 Nagamatsu, S., Nakamichi, Y., Watanabe, T., Matsushima, S., Yamaguchi, S., Ni, J., Itagaki, E. and Ishida, H. (2001) Localization of cellubrevin-related peptide, endobrevin, in the early endosome in pancreatic β cells and its physiological function in exo-endocytosis of secretory granules. J. Cell Sci. **114**, 219–228
17 Oheim, M., Loerke, D., Stuhmer, W. and Chow, R. H. (1998) The last few milliseconds in the life of a secretory granule. Docking, dynamics and fusion visualized by total internal reflection fluorescence microscopy (TIRFM). Eur. Biophys. J. Biophys. Lett. **27**, 83–98
18 Schmoranzer, J., Goulian, M., Axelrod, D. and Simon, S. M. (2000) Imaging constitutive exocytosis with total internal reflection fluorescence microscopy. J. Cell Biol. **149**, 23–31
19 Landis, D. M., Hall, A. K., Weinstein, L. A. and Reese, T. S. (1988) The organization of cytoplasm at the presynaptic active zone of a central nervous system synapse. Neuron **1**, 201–209
20 Garner, C. C., Kindler, S. and Gundelfinger, E. D. (2000) Molecular determinants of presynaptic active zones. Curr. Opin. Neurobiol. **10**, 321–327
21 Fernandez, J. M., Neher, E. and Gomperts, B. D. (1984) Capacitance measurements reveal stepwise fusion events in degranulating mast cells. Nature (London) **312**, 453–455
22 Wasmeier, C. and Hutton, J. C. (1996) Molecular cloning of phogrin, a protein-tyrosine phosphatase homologue localized to insulin secretory granule membranes. J. Biol. Chem. **271**, 18161–18170
23 Pouli, A. E., Karagenic, N., Arden, S., Bright, N., Schofield, G. S., Hutton, J. C. and Rutter, G. A. (1998) A phogrin–aequorin chimaera to image free Ca^{2+} in the vicinity of secretory granules. Biochem. J. **330**, 1399–1404
24 Tabb, I., Kish, P. E., Van Dyke, R. and Ueda, T. (1992) Glutamate transport into synaptic vesicles. Roles of membrane potential pH gradient and intravesicular pH. J. Biol. Chem. **267**, 15412–15418
25 Sankaranarayanan, S. and Ryan, T. (2001) Calcium accelerates endocytosis of vSNAREs at hippocampal synapses. Nat. Neurosci. **4**, 129–136
26 Gad, H., Low, P., Zotova, E., Brodin, L. and Shupliakov, O. (1998) Dissociation between Ca^{2+}-triggered synaptic vesicle exocytosis and clathrin-mediated endocytosis at a central synapse. Neuron **21**, 607–616
27 Schmid, S. L., McNiven, M. A. and DeCamilli, P. (1998) Dynamin and its partner: a progress report. Curr. Opin. Cell Biol. **10**, 504–512

Received 22 August 2001/10 December 2001; accepted 24 January 2002